







# An Earthquake Early Warning System for Northern Chile Based on ElarmS-3

Miguel Medina<sup>1</sup>, Rodrigo Sanchez<sup>1</sup>, Sebastián Riquelme<sup>1</sup>, Maria C. Flores<sup>1</sup>, Pablo Koch<sup>1</sup>, Francisco Bravo<sup>1</sup>, Sergio Barrientos<sup>1</sup>, Ivan Henson<sup>2</sup>, Angela Chung<sup>2</sup>, Diego Melgar<sup>3</sup>, Constantino Mpodozis<sup>4</sup>, Margaret Hellweg<sup>2</sup>, and Richard Allen<sup>2</sup>

## Abstract

During 2020, the National Seismological Center (CSN) implemented an earthquake early warning system (EEWS) for northern Chile. From a seismological point of view, this area is considered to be one of the largest seismic gaps in Chile, where an  $M_w \sim 9.0$  earthquake is expected in a region with a population of more than 1.4 million people. From an economical perspective, this region holds 90% of the copper mining companies in Chile, with more than 15% of the Gross National Product coming from the mining industry. Antofagasta Minerals funded an EEWS prototype for this region with the purpose of keeping both the population and the mining industry safe; 25 new seismic stations have been added to the CSN permanent network to develop an EEWS capable of issuing strong shaking alerts, which could potentially save lives and support critical mining operations in the region. During a 20 month period, we successfully detected, located, and calculated the magnitude of 1774 earthquakes (0–300 km depth) using ElarmS-3, an earthquake early warning algorithm from the University of California, Berkeley. The alert time, or the time between when an earthquake alert is issued and the S-wave arrival at the location, is on average  $\sim 24$  s, and 96% of shallow and intermediate depth earthquakes (0–150 km) with  $M \geq 5.0$  were alerted. We obtained errors of  $0.52 \pm 0.43$  in magnitude,  $30.4 \pm 42.72$  km in location,  $43.5 \pm 50.0$  km in depth, and  $6.6 \pm 10.6$  s in origin time.

**Cite this article as** Medina, M., R. Sanchez, S. Riquelme, M. C. Flores, P. Koch, F. Bravo, S. Barrientos, I. Henson, A. Chung, D. Melgar, et al. (2022). An Earthquake Early Warning System for Northern Chile Based on ElarmS-3, *Seismol. Res. Lett.* **93**, 3337–3347, doi: [10.1785/0220210331](https://doi.org/10.1785/0220210331).

[Supplemental Material](#)

## Introduction

Northern Chile (17–26° S) is considered to be one of the largest and most mature seismic gaps in the world, where a megathrust earthquake ( $M_w \sim 9.0$ ) could take place in the near future (Béjar-Pizarro *et al.*, 2013; Hayes *et al.*, 2014; Metois *et al.*, 2016). By written record, the largest known earthquake in this region is the 1877  $M_w$  8.8 earthquake (Comte and Pardo, 1991; Lomnitz 2004), and since this massive event, an extended seismic quietness was only disturbed in 2014 by the  $M_w$  8.1 Iquique earthquake (Ruiz *et al.*, 2014). This event was not able to cover the massive seismic gap, and therefore it is still possible for a large megathrust earthquake to take place in this area in the near future.

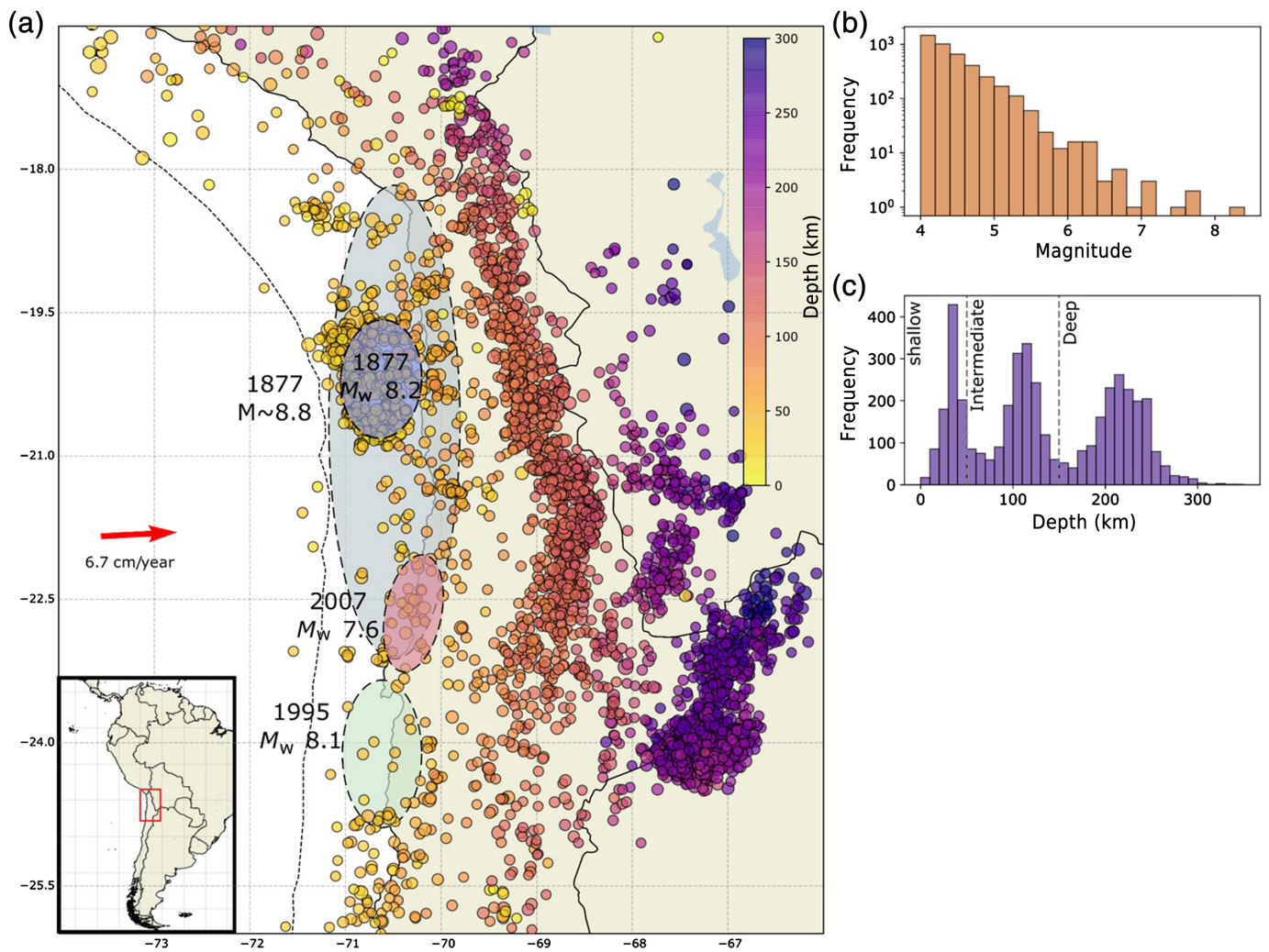
We can classify this region's seismicity by its depth in three main groups: shallow earthquakes, intermediate depth earthquakes, and deep earthquakes. As seen in Figure 1, shallow earthquakes (0–50 km) are mostly interplate events along the coast, as well as shallow seismic activity inside the Nazca plate below the megathrust. A minority of them are located inland related to faulting along the Andes Mountain range. Historically, shallow interplate events are the largest ones and include the earthquakes in 1877 ( $M_w$  8.8) and

2014 ( $M_w$  8.1); this is also true for the majority of Chilean seismicity. Intermediate depth earthquakes (50–150 km) or intra-plate earthquakes are the most common group of earthquakes in this region and are usually of moderate magnitude ( $M < 6.0$ ). Although large intraplate earthquakes are not as common as interplate earthquakes (Ruiz and Madariaga, 2018), two large intermediate depth events occurred in this region at similar depths ( $\sim 100$  km): 1950  $M_w \sim 8.0$  Calama (Kausel and Campos, 1992) and 2005  $M_w$  7.7 Tarapacá (Peyrat *et al.*, 2006). Deep events (150–300+ km) are frequent in this region (see Fig. 1), which is not the case for most of the Chilean territory (Ruiz and Madariaga, 2018; Derode and Campos, 2019). These events are usually of moderate magnitude

1. National Seismological Center, Faculty of Physical and Mathematical Sciences, University of Chile, Santiago, Chile, <https://orcid.org/0000-0002-1722-1075> (MM); <https://orcid.org/0000-0002-5271-7375> (MCF); <https://orcid.org/0000-0001-8806-9077> (FB); 2. UC Berkeley Seismological Laboratory, University of California, Berkeley, California, U.S.A., <https://orcid.org/0000-0002-3767-6018> (AC); <https://orcid.org/0000-0003-4293-9772> (RA); 3. Department of Earth Sciences, University of Oregon, Eugene, Oregon, U.S.A., <https://orcid.org/0000-0001-6259-1852> (DM); 4. Antofagasta Minerals S.A., Santiago, Chile

\*Corresponding author: [mmedina@csn.uchile.cl](mailto:mmedina@csn.uchile.cl)

© Seismological Society of America



( $M < 6.0$ ) and go mostly unnoticed by the majority of population because they take place below the Andes Mountain range, which is sparsely populated and seismic amplitudes are highly attenuated by rising magma under the arc and the mantle wedge. No large ( $M > 8.0$ ) deep earthquake has been recorded in Chile (Ruiz and Madariaga, 2018).

This northern section of the country is also of notable economical interest, for it hosts most of the copper mining related activity with about 90% of the total country operations located there, making it an important part of Chile's gross national product directly related to the mining industry. Furthermore, Iquique and Arica, two of the major ports in Chile, are also located in this region.

In a region with such a wide variety of earthquakes and economical significance, tools for delivering relevant information to decision makers, such as an earthquake early warning system (EEWS) that could alert nearby population before they feel strong shaking, are of great importance. EEWS have been implemented around the world in different regions (Allen and Kanamori, 2003; Allen *et al.*, 2009; Hsiao *et al.*, 2009; Kamigaichi *et al.*, 2009; Satriano *et al.*, 2011; Chung, *et al.*,

**Figure 1.** Northern Chile region, historical, and recent seismicity. (a) National Seismological Center (CSN) catalog seismicity ( $M \geq 4.0$ ) distribution during 2013–2021. Dotted ellipses represent approximate rupture areas for large historical and recent earthquakes in Chile. The inset shows Northern Chile's location in South America. (b) Magnitude and (c) depth distribution for the CSN 2013–2021 seismicity catalog ( $M \geq 4.0$ ) in this region. The color version of this figure is available only in the electronic edition.

2019; Cremen and Galasso, 2020; Kurzon *et al.*, 2020; Brooks *et al.*, 2021; Massin *et al.*, 2021) with distinct methodologies and outcomes adapted to each country's reality. Though some methods have been implemented and tested in Chile, such as a smartphone-based system (Finazzi and Fasso, 2017), Geodetic First Approximation of Size and Timing (Crowell *et al.*, 2018), FinDer version 2 (v.2; Böse *et al.*, 2018), and recently Machine Learning Assessed Rapid Geodetic Earthquake (Lin *et al.*, 2021), no EEWS has been in operation for a long, continuous period of time.

To improve the overall response for such big earthquakes in the region, a joint effort was made between the National

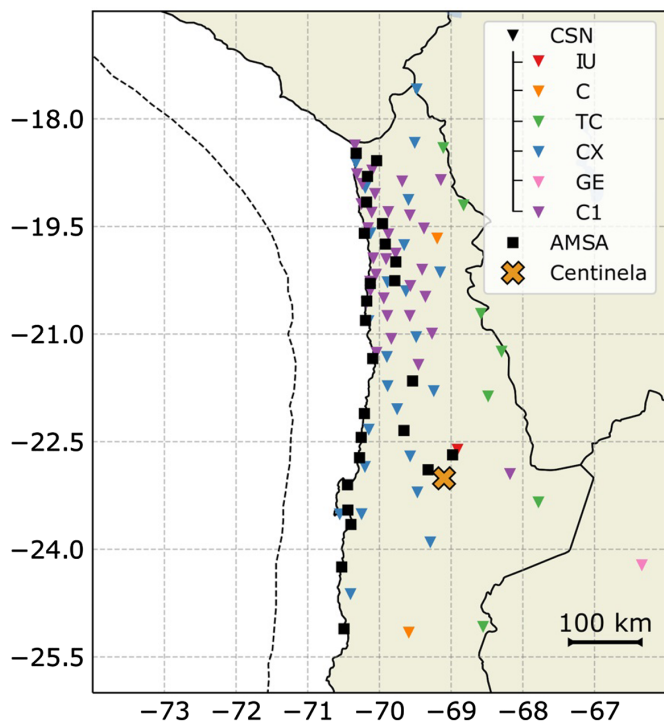


**Figure 2.** Current Northern Chile seismological station network. Triangles represent the existing station network (denoted as CSN), in which each color indicates its parent network, detailed in the Introduction section. The newly installed stations are in squares and are part of the Antofagasta Minerals (AMSA) network. The CSN network consists of strong-motion and/or broadband stations, and the AMSA network only uses broadband stations. The orange cross marks the Centinela Mining District. The color version of this figure is available only in the electronic edition.

Seismological Center (CSN) and Antofagasta Minerals (AMSA) to develop an EEWS for northern Chile that is capable of issuing strong shaking alerts for earthquakes.

With AMSA's financial support, an additional 25 broadband seismometers were added to this region's current seismic station network, which consists of 68 multiparameter stations from various networks, including the Global Seismograph Network—Incorporated Research Institutions for Seismology/U.S. Geological Survey (IU), IPOC Seismic Network (CX), Observatorio Volcanológico de los Andes del Sur (TC), Red Sismológica Nacional (C1), Chilean National Seismic Network (C), and GEOFON/Instituto Nacional de Prevención Sísmica (INPRES) (GE). This array of 68 stations can be seen in the triangles in Figure 2 and will be referred to as the CSN network hereafter. The CSN network is composed of a variety of broadband and strong-motion stations; some stations contain both, in which case ElarmS-3 uses both as an input. The 25 newly installed stations will be referred to as the AMSA network hereafter and can be seen in the squares in Figure 2. During February–March 2020, the AMSA network was installed along the northern Chilean coast (see Fig. 2), with

stations starting to record and transmit seismic data in that period. Stations were mostly placed near the coast for telecommunication purposes and to improve coverage for interplate earthquakes.

In addition, a rapid estimation of earthquake magnitude and location is obtained in real time using ElarmS-3 (Chung *et al.*, 2019), an EEWS. Strong-motion alerts are then broadcasted at predefined locations including CSN and key mining operations, such as the Centinela Mining Complex (see Fig. 2).

With current operation in CSN, using ElarmS-3, we are able to obtain reliable solutions, within an expected margin of error, and issue alerts in the first seconds following an earthquake, before preliminary solutions can be obtained with traditional methodologies (Barrientos and National Seismological Center [CSN] Team, 2018). At this time, alerts are delivered to decision makers in AMSA. ElarmS-3 is operated as a separate independent platform in CSN.

In this work, we describe the development of the present EEWS in northern Chile as well as the results that have been obtained through the 20-month period from March 2020 to October 2021.

## Methods and Data

Our current EEWS consists of utilizing ElarmS-3 to quickly characterize an event's magnitude and location using data from stations in the network. Strong motion or S-wave arrival times are subsequently computed, and an earthquake alert is delivered to decision makers at predefined key locations. Earthquake alerts are displayed in a web server with relevant information such as earthquake magnitude, distance to the epicenter, and a decreasing timer with expected strong-motion time at the location. Recent earthquake alert information can also be examined in a custom graphical user interface (GUI).

Rapid estimation of earthquake parameters such as magnitude, hypocentral location, and origin time are obtained using ElarmS-3 (Allen 2007; Chung *et al.*, 2019). Earthquake magnitude is obtained using the P-wave amplitude at near stations following ElarmS methodology (Kuyuk *et al.*, 2014; Chung *et al.*, 2019). A first earthquake alert is issued when a trigger is identified in four stations, using the first 4 s of data with a short-term average/long-term average (STA/LTA) picker on high-pass-filtered vertical components. After this first alert, earthquake parameters are constantly updated and become more accurate as waves reach further stations and more seismic data are available. Only earthquake parameters for this first alert are used to compare the CSN earthquake catalog and our EEWS solutions.

Our workflow for adapting ElarmS-3 to the Chilean subduction consists of defining a preliminary earthquake catalog to test the system; using an adapted local wave velocity model (Dziewonski and Anderson, 1981; Husen *et al.*, 1999) for earthquake location and strong-motion arrival estimation; establishing a range of possible earthquake depths; identifying



system latencies and earthquake parameter uncertainties; and introducing newly installed seismic stations. Detailed information on these catalogs, tests, and modifications are described in the following paragraphs.

During early 2020, several preliminary tests were carried out to adapt ElarmsS-3 to the subduction related seismicity in Chile. These tests were performed using an earthquake catalog consisting of 395 events recorded by CSN between January 2013 and February 2020, with magnitude  $\geq 5.0$  in northern Chile between  $16.5^{\circ}$ – $26^{\circ}$  S and  $66^{\circ}$ – $74^{\circ}$  W. A 210 s long window was extracted for each event at every available station at the time, including 10 s before the origin time (O.T.) and 200 s after the O.T., a long enough window for stations to capture relevant information and the EEWS to issue a realistic warning. Seismic data were processed simulating real-time operation. We included a 1 s simulated latency to account for telemetry delay, which can be as great as 2–3 s in most cases.

Strong-motion alerts corresponding to the *S*-wave arrival are computed and broadcast at predefined locations including CSN and key mining complexes. These values are calculated using ray-path modeling with an adapted local wave velocity model. This model uses a widely applied local model for the region (Husen *et al.*, 1999) for the first 0–80 km, and deeper values are obtained from the preliminary reference Earth model (Dziewonski and Anderson, 1981).

Once an earthquake is located and an alert is issued, estimated arrival times for strong-motion waves are communicated and displayed to decision makers at predefined mining locations using a web server with a custom Earthquake Alert GUI (available in the supplemental material to this article).

The time between when an alert is issued and when an *S*-wave arrives at a location is defined as the alert time and corresponds to the period of time when critical decisions can be made. System latency or alert latency, on the other hand, is the time that the EEWS takes to issue an alert since the O.T. and encompasses telemetry delays, wave processing, alert computing, and delivery time. As such, system latency accounts for seismic-wave travel time from an earthquake source to at least four stations and by its own nature is directly related to station density around the event. Computing time starts when data are available from at least one station and stops when an alert is issued; it is mostly related to station data availability because in-system alert computing is near automatic when seismic data are available. A schematic diagram for these concepts can be seen in Figure 3a. In addition, a flowchart for the EEWS can be seen in Figure 3b, which details an overview for the functioning of our system.

As previously mentioned, there is a large variation in depths and locations of earthquakes seen in northern Chile, meaning that we could not correctly locate earthquakes using a grid search with a single fixed depth value, as we tested in our first approach. After subsequent extensive testing, we settled on the best model of possible depths to describe this subduction zone:

2, 4, 8, 12, 16, 20, 30, 40, 50, 65, 80, 100, 120, 140, 160, 180, 200, 250, and 300 km. We observed the best congruence between our initial CSN solution and the obtained hypocentral locations when using this variable depth model similar to the one used for Japan subduction earthquakes by Meier *et al.* (2020). Other modifications included but were not limited to values such as STA/LTA thresholds and minimum and maximum values for earthquake motion, among others. These values changed over time as more stations were available and more data were collected.

After we were done with our preliminary testing, during February–March 2020, the new AMSA network was deployed to improve station density in northern Chile, as seen in Figure 2. This new network is composed of 25 triaxial broadband seismometers (Trillium Compact 120s) that transmit data in real time. This new network implies a 37% increase in total stations and a 12% decrease in overall station spacing, this being the mean distance between any station and its nearest station.

Concurrent with the installation of the new AMSA network during early 2020, real-time operation began in March 2020 once preliminary testing was complete, and a baseline for detectability was defined. We analyze results for the March 2020–October 2021 period. Obtained hypocentral solutions and magnitudes for alerts issued are compared with CSN manually revised solutions for magnitudes 3.0 and above, for which the CSN catalog is considered to be complete in the area. The *S*-wave arrival time and error in this prediction (observation–prediction) are computed at the Centinela Mining District with observed data at this location.

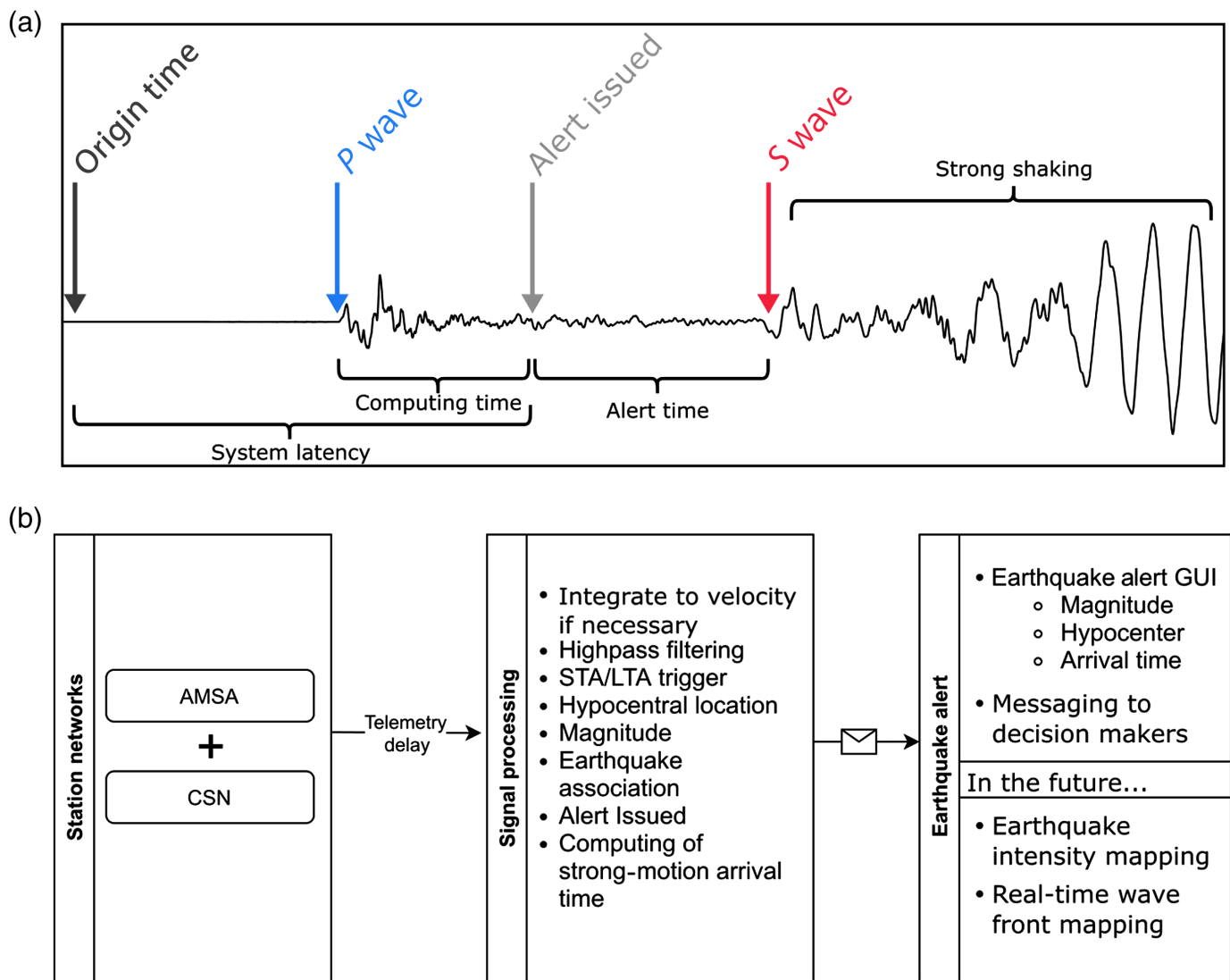
## Results

The EEWS performance was suitable after preliminary tests and modifications were done, with 83% of events in the catalog ( $M \geq 5.0$ ) issuing an alert. Mean absolute magnitude errors of 0.8 units, horizontal location error of 53.5 km, depth errors of 55.3 km, and origin time errors of 8 s were obtained in the predicted earthquake source versus CSN location. This was determined as our baseline for earthquake detection going forward to introduce real-time operation.

The two largest earthquakes that we could analyze in this region catalog belonged to the same sequence in 2014 (Ruiz *et al.*, 2014): the 1 April 2014  $M_w$  8.1 mainshock and its largest aftershock two days later ( $M_w$  7.6). For the mainshock, an  $M_w$  6.5 alert was issued 23 s after the O.T. with an alert time of 38 s, with an error of 1.6 magnitude units, epicentral error of 7 km, and 22 km in depth. Similar results were obtained for the aftershock; an  $M_w$  5.8 alert was issued with a similar time of 24 s after the O.T. and 22 s of alert time, with 1.8 magnitude units of error, 14 km of epicentral error, and 6 km in depth.

During the following 20 months (March 2020–October 2021), we saw a similar performance in the real-time operation. Although software was still being tweaked, operations remained stable. A total of 1774 alerts associated with earthquakes were





issued; EEWS event location in relation to CSN manually revised location can be seen in Figure 4. Errors in Figure 4 are calculated as observation–prediction.

These 1774 alerts accounted for 93% of the earthquakes with magnitude  $M \geq 5.0$ , 72% for  $M \geq 4.0$ , and 52% for  $M \geq 3.0$  (see Table 1). Several alerts were issued for  $M < 3.0$  events, but those are not listed because they are not usually reported by the CSN.

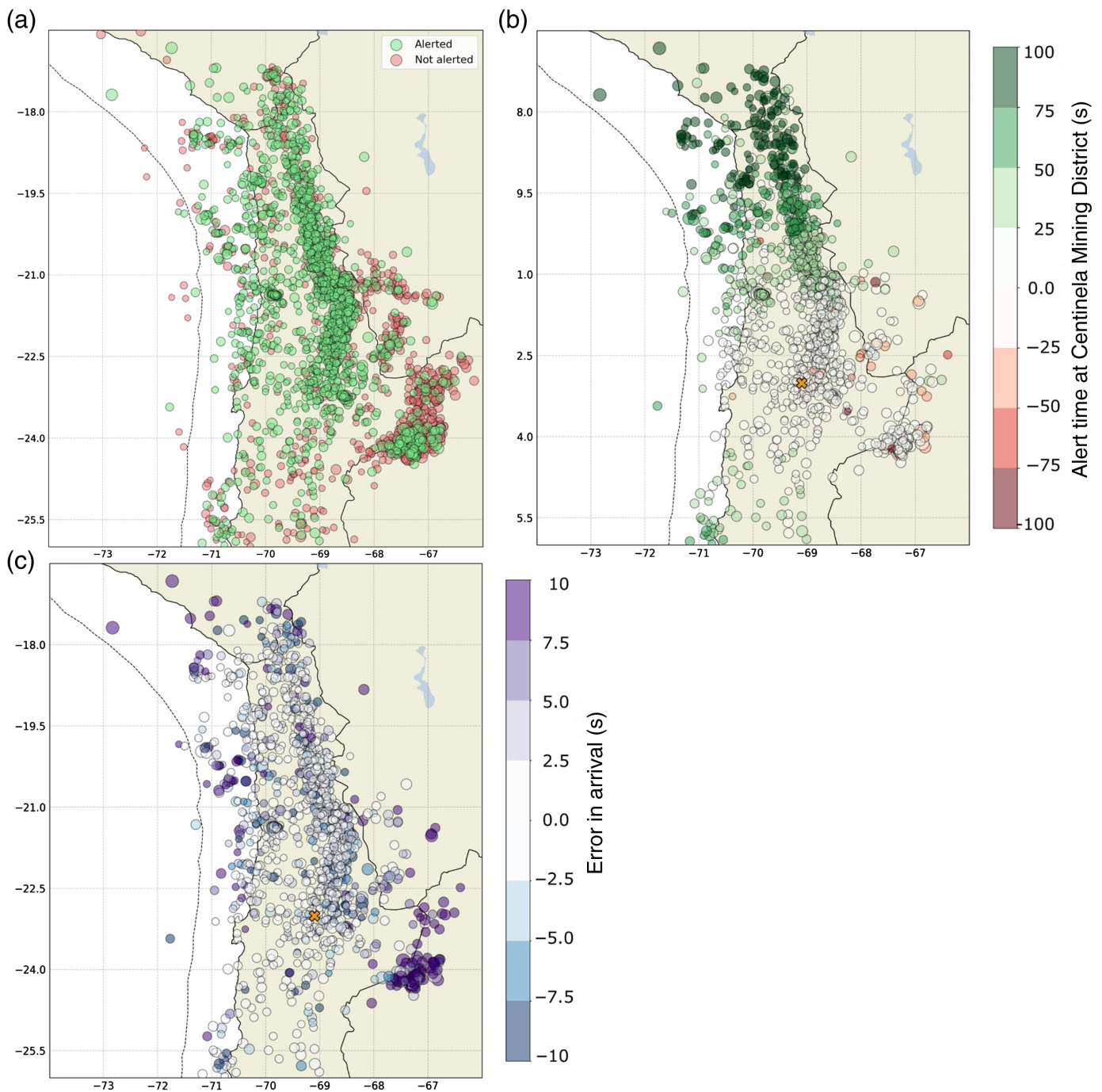
Discrepancies between preliminary (EEWS) and reported (CSN) locations and magnitudes (observation–prediction) can be seen in Figure 5. In the period from March 2020 to October 2021, we observed mean absolute magnitude errors of 0.52 ( $\sigma = 0.43$ ), horizontal location error of 30.4 km ( $\sigma = 42.72$ ), depth errors of 43.5 km ( $\sigma = 50.0$ ), and origin time errors of 6.6 s ( $\sigma = 10.6$ ). These high values for deviation are related to highly dispersed distributions.

Alerts are issued within 4 s of the *P*-wave arriving at four stations for 90% of the events. Mean alert latency times (time since the O.T.) are 17 s for shallow seismicity, 22.8 s for intermediate events, and 32.3 s for deep earthquakes. Mean alert

**Figure 3.** Schematic earthquake early warning system (EEWS) operation. (a) Example of an earthquake detection and strong-motion alert being issued. System latency accounts for time elapsed since the origin time (O.T.) until an alert is issued. (b) Flowchart for EEWS functioning divided into station network, signal processing, and earthquake alert. GUI, graphical user interface; STA/LTA, short-term average/long-term average. The color version of this figure is available only in the electronic edition.

times at Centinela are 24 s for all earthquakes, with 43.1 s, 23.3 s, and 5.7 s for shallow, intermediate, and deep earthquakes, respectively.

There was a total of 1617 missed or nonalerted events. These missed events are made up of 1414 events between magnitude 3.0 and 4.0 or 52% of the total events in this range, 200 between 4.0 and 5.0 (30%), 3 between 5.0 and 6.0 (7%), and none with magnitude 6.0 and above (0%). By depth we see that, of the total of missed alerts, 170 or 11% of these are shallow events (0–50 km), 569 or 35% are intermediate (50–150 km), and 878 or 54% are deep events (150+ km).



## Discussion

Though preliminary results using the 2013–2020 catalog were low on overall detectability, these values were expected to be a lower bound when compared with real-time operation because the seismic network had improved through the years (Barrientos and National Seismological Center [CSN] Team, 2018; Riquelme *et al.*, 2018), and for some analyzed events the number of available stations was drastically reduced compared with the current network, particularly for deeper events or events prior to 2015–2016.

Conversely, alerts issued that replay catalog seismic data are expected to be slightly faster than those issued in real time, for

**Figure 4.** EEWS operation during March 2020–October 2021. (a) Seismicity distribution for earthquakes with and without an alert issued. (b) Alert time in the Centinela Mining District for all detected earthquakes. (c) Error in prediction (observation–prediction) of earthquake strong-motion wave arrivals in the Centinela Mining District. The orange cross marks the Centinela Mining District. The color version of this figure is available only in the electronic edition.

the former do not account for realistic telemetry latencies or for delay in alert distribution. Though a 1 s simulated telemetry latency was included in our testing across all stations, real

TABLE 1

**Earthquake Early Warning System (EEWS) Detection Thresholds by Period of Time, Seismicity Depth, and Magnitude**

Magnitude Range	Total Number of Events Registered	2020–2021	2020–2021 (Depth ≤ 150)	Only 2021	Only 2021 (Depth ≤ 150)
M ≥3.0	3391	52%	68%	57%	76%
M ≥4.0	582	72%	90%	76%	95%
M ≥5.0	40	93%	96%	100%	100%
M ≥6.0	7	100%	100%	100%	100%

The 2020–2021 period includes March 2020–October 2021. The 2021 period includes seismicity in January–October 2021.

telemetry latencies are not constant and can fluctuate mostly between 1 and 3 s and more in some particular instances.

Changes made to the ElarmS-3 configuration greatly increased the detectability of earthquakes in the northern Chilean territory. When compared with our initial results, this first implementation of an autonomous EEWS has been overall satisfactory. Further changes will be required to improve magnitude uncertainty and preliminary hypocentral locations, but as it stands, current alerts are suitable. For fast and reliable solutions in each site, and also for redundancy purposes, identical signal processing is done both in CSN and in the Centinela Mining Complex independently. Slight differences in solutions are mostly neglectable and are associated with telecommunication discrepancies that may increase some stations latencies at each site.

As seen in data for our first year (see Fig. 5), estimated magnitudes are overall biased to be lower than those reported by the CSN catalog, but the opposite happens for the smaller events. In Figure 5e, we observe that magnitude errors for larger earthquakes tend to be smaller and thus are estimated more accurately. It is also important to consider that we compare the first version of the obtained earthquake parameters, and these values are updated as more stations become available, making them subsequently more accurate. Nevertheless, for earthquake early warning purposes, these errors are adequate, considering that fast and reliable earthquake locations are obtained with acceptable magnitude errors. In the future, we expect to improve our location and magnitude estimation with further revisions to help alleviate this issue.

We consider in more detail two events of considerable magnitude and shaking at the Centinela Mining District. We observe the 3 June 2020  $M_w$  6.9 07:35:34 UTC with a depth of 123.4 km and at a 68.4 km epicentral distance with respect to the mining district. This event had a magnitude error of 0.1 units and an epicentral error of 4.2 km, but due to its proximity, it only had about 5 s of alert time. On the other hand, the 11 September 2020  $M_w$  6.3 event 07:35:56 UTC with a depth of 54.4 km at a 203.6 km epicentral distance had a magnitude error of  $-0.4$  units and an epicentral error of 9.7 km, but it had about 23 s of alert time when the shaking

alert was issued. In both cases, moderate to strong shaking was reported at the Centinela Mining District with peak ground accelerations of  $\sim 0.13g$  and  $\sim 0.04g$  for the  $M_w$  6.9 and 6.3 events, respectively.

The inclusion of a set of 19 possible depths for earthquake solutions improved our preliminary location greatly. We settled on using a denser model near the surface because we usually have a finer resolution for shallow events compared with deeper earthquakes. As a result, this EEWS is capable of issuing alerts for an important fraction of the events that take place every year in this region. The obtained result of alerts for 93% of the total events are in line with those obtained by other authors using much denser station networks in both different and similar tectonic settings (Chung *et al.*, 2019; Meier *et al.*, 2020).

As such, this current implementation for an EEWS is adequate for shallow and intermediate depth earthquakes, with 96% of the events with  $M \geq 5.0$  having alerts issued. As seen in Figures 4 and 5, alerts for deeper earthquakes are not reliable in northern Chile with the current CSN and AMSA network distribution. However, these events are usually not reported to have been felt by the general public because they occur in areas sparsely populated.

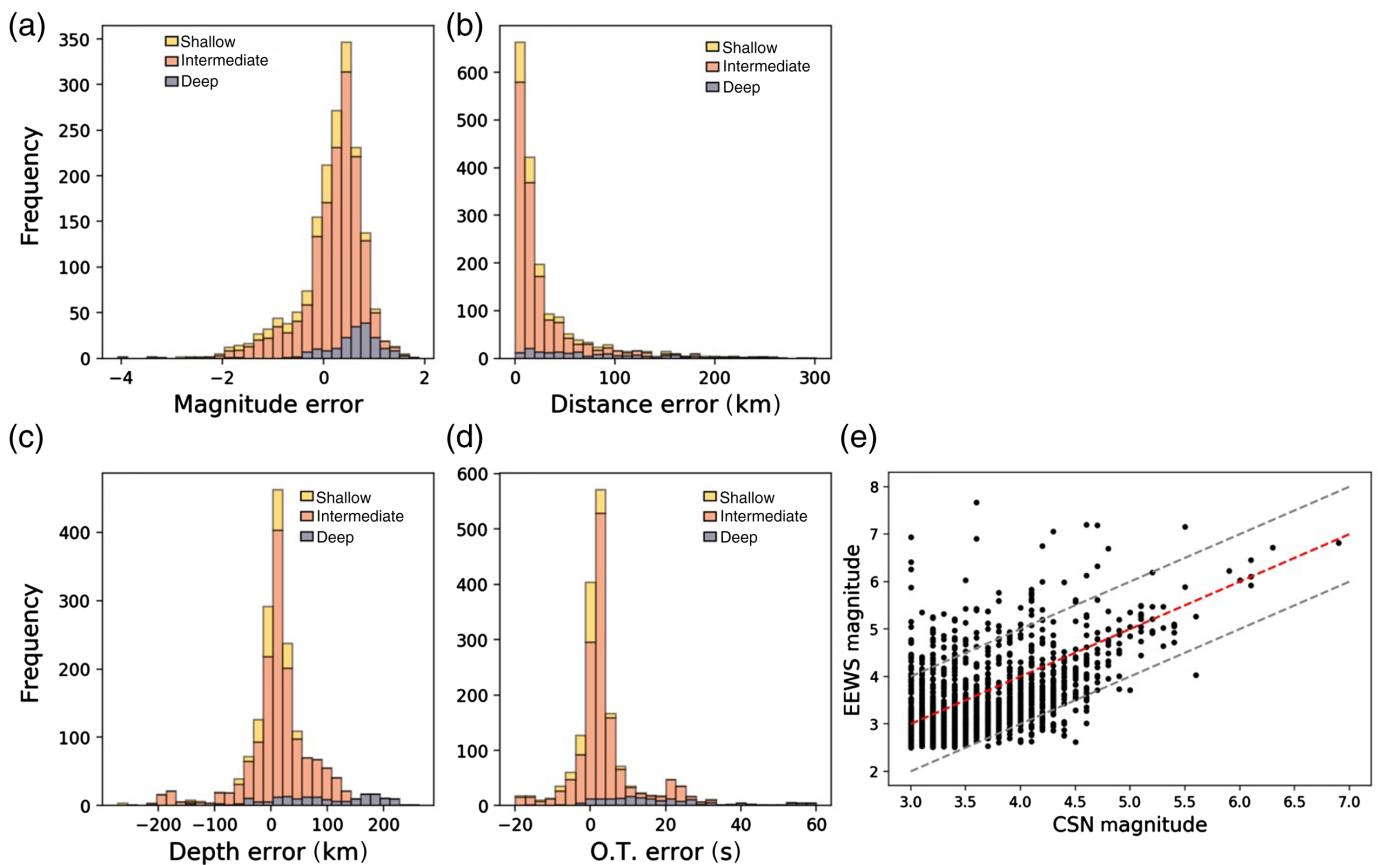
We expect the system to behave well under a major offshore shallow interplate earthquake, with alert times similar or lower than those observed in the 2014  $M_w$  8.1 Iquique earthquake.

Deeper events are difficult to locate quickly, taking place below the Andes Mountain range in an area with low station density, difficult terrain, and poor telecommunication capabilities. With no stations nearby, seismic waves travel through terrain faster than the system can locate them and therefore fall into a blind zone of the EEWS.

This EEWS is not suited for detecting slow earthquakes or tsunami earthquakes because these do not generate great shaking and the system would most likely greatly underestimate their magnitude. In addition, specialized tools such as *W*-phase are in place at CSN for such instances (Riquelme *et al.*, 2018).

As seen in Figure 4b, events taking place near the Centinela Mining District have lower alert times as opposed to those far away, as to be expected. We observe that events at a 0–75 km distance have a mean 0 s alert time, events between 75–150 km





have a mean 5.4 s of alert time, and events at 150–200 km have a mean 14.3 s of alert time. This indicates that we have an approximately 75 km radius blind zone in which events occurring cannot be alerted on time. To increase alert times, alert latency time needs to be lowered and more stations are needed because computing times are mostly bound by seismic station data availability at four or more stations.

With the current operation, alert times for earthquake strong motion could theoretically be 20 or more seconds in 785 instances for the Centinela Mining District, as seen in Figure 4. This might be enough for some safety measures to be applied or critical operations to be stopped. In particular at this location, in preliminary testing, we obtained an alert issued 38 s before the S-wave arrival for the 2014  $M_w$  8.1 Iquique earthquake and 22 s for its mainshock ( $M_w$  7.6). No data for ground shaking at this location were available at the time.

As a side note, in testing we found that we were unable to detect any earthquake that took place an hour after the 2014  $M_w$  8.1 Iquique mainshock, even for those with a magnitude between 4.0 and 5.0. This directly relates to the STA/LTA picker algorithm being unable to identify events inside the remainder body waves of the mainshock and is something that has to be taken into account when dealing with large megathrust events in real time. This could prove problematic if a large foreshock took place right before an even larger mainshock; however, in this particular instance, we do expect the first alert to reach decision makers.

**Figure 5.** Error (observation–prediction) distribution histograms for (a) magnitude, (b) horizontal or epicentral distance, (c) depth, and (d) origin time. (e) Comparison between CSN catalog magnitude and earthquake early warning prediction. The red central line is a 1:1 ratio, and gray lines represent errors  $\pm 1.0$  in magnitude units. The color version of this figure is available only in the electronic edition.

Earthquakes occurring inside the station network are much more likely to be identified quickly and correctly as opposed to those occurring out of network, such as offshore earthquakes or deep events, and this directly relates to the way ElarmS-3 tries to locate an earthquake using one station as a reference point. Nevertheless, offshore interplate earthquakes are efficiently alerted because they take place fairly close to the coast and do not affect the algorithm (as opposed to outer-rise events or deep events), but they have greater uncertainties reflected mostly in epicentral location errors. On the topic of out-of-network events, ElarmS-3 uses a teleseismic filter, and we did not trigger any teleseismic events during our operation.

Improving the current station network density is likely to be the single most important change for reducing earthquake system latency and enhancing alert times, barring having stations offshore. This is exemplified by Chung *et al.* (2019) who showed some remarkably fast solutions for earthquake detection using ElarmS-3 in areas where station spacing was close to

10 km. By comparison with our current CSN + AMSA network, spacing is much closer to 30 km.

A possible reasonable alternative to densify our current station network would be to use low-cost seismic stations such as the Raspberry Shake (Anthony *et al.*, 2019). Similar low-cost stations have been tested by the CSN south of the area of study in this work using an identical EEWS, and we have seen substantial improvements in earthquake detection and alert latency for earthquakes bigger than  $M_w \sim 4.5$ . Although these stations have larger signal-to-noise ratios and thus usually have bigger uncertainties, the sheer number of stations that can be deployed would most likely overcome this setback and should not be an issue for larger earthquakes ( $M \gtrsim 7.0$ ).

Although real-time operation began in March 2020, the deployment of the EEWS was impaired by the COVID-19 pandemic; major difficulties in Chile also began in March 2020 and impacted everyday operations of the CSN (Barrientos *et al.*, 2021). Lockdowns affected maintenance work and deployment of some stations in the area. Nonetheless, the core structure for a functional system was able to be put in place in spite of the difficulties, and real-time operation has remained mostly unscathed.

Occasionally, false alarms do happen as a result of the EEWS flagging *S* waves as *P* waves and generating a new duplicated event. Though ElarmS3 can mostly automatically filter these occurrences, when they do happen, they are flagged as duplicate events by the EEWS GUI using a time and location filter. Nevertheless, we have seen a handful of instances when false alarms managed to slip through these filters due to an irregular location of the duplicated event. In one instance an  $M > 5.0$  event alert that never took place was issued, probably related to an error in telecommunications. Similarly, as can be seen in Figure 5a,b, there are a few instances in which a small event ( $M < 2.0$ ) triggered a higher magnitude ( $M \sim 5.0$ ) alert (magnitude error  $> 3.0$ ) due to being coupled to a faulty epicentral location (error  $> 200$  km); these instances have been corrected and have not taken place in the past year.

Changes to alerts that we currently display and communicate to decision makers are being considered as we identify possible weaknesses and areas of improvements in our system. More personalized alerts, as well as broadcasting of these warnings to a more generalized audience, are a high priority. In addition, displaying detailed information such as expected ground-motion intensity and real-time wavefront propagation is currently being worked on to be implemented in the near future.

On a final note, seldomly, events reported by the EEWS take place in Argentina and are not reported by the CSN unless felt by observers in Chile. These nonreported event alerts are frequently manually checked against information reported by the Argentinian INPRES. Agreement is similar to that obtained with events inside the Chilean territory, but these results are not shown in this work because the nature of this nonautomatic revision is partial and not exhaustive.

## Conclusions

The proposed EEWS shows appropriate results for shallow and intermediate depth earthquakes (0–150 km), with acceptable hypocentral location errors and magnitude errors and alerts issued for 96% of these events with  $M \geq 5.0$ . Deeper events (150+ km) are hard to locate quickly because they take place below areas with difficult to access terrain (Andes Mountain range) and therefore are likely to have low station density around them. With no stations nearby, waves travel through the terrain too fast for the system and therefore fall into a blind zone of the EEWS, making them not suitable for this EEWS.

An earthquake alert is issued when a trigger is identified in four stations, using the first 4 s of data with an STA/LTA picker. We observe 14.3 s of alert for events occurring at a 150–200 km distance in the Centinela Mining District. The mean alert time at this location is 24 s for the entirety of the northern Chile seismicity.

With no other system in place for early earthquake alerts of this scale in Chile, the significance of this EEWS is enhanced, and this endeavor could greatly improve our response to large megathrust earthquakes and in the future could be available to the general public. This project could also be scaled to include other regions of Chile to improve coverage, but this end goal is closely related to the deployment of a denser station network all throughout the Chilean territory.

Future work will include broadcast of more detailed information for earthquake alerts, such as visualizing wavefront propagation in real time, providing expected ground-motion intensity at each location with an associated shake map, and improving the earthquake location and magnitude estimation, which is one of our main areas in need of improvement. A trade-off between expected event magnitude and alert recipient distance is being tested for issuing alerts to not alert for moderate events in a huge area, but no concrete values have been decided yet. Furthermore, we recognize the importance of more personalized alerts, and a series of alternatives are being considered, for instance texting via an short message service Gateway. For testing purposes, we have implemented an initial trial of smartphone alerts using Telegram application programming interface for a small number of participants; it has been widely successful with no significant delays recorded. An official channel of communication would streamline alerts being deployed for the general public.

## Data and Resources

Seismic data used in this study were collected by the National Seismological Center ([www.csn.uchile.cl](http://www.csn.uchile.cl)). Seismic data from Instituto Nacional de Prevención Sísmica (<https://www.inpres.gob.ar>) were used to validate earthquakes in Argentina. All the websites were last accessed in November 2021. The supplemental material for this article includes an example for the custom graphical user interface displaying earthquake alerts.

## Declaration of Competing Interests

The authors acknowledge that there are no conflicts of interest recorded.

## Acknowledgments

The authors would like to thank the UC Berkeley team for help with setting up the earthquake early warning system in the initial stages, Antofagasta Minerals for providing financial support to enhance the region's seismological network, and the National Seismological Center team and the National Office of Emergency of Chile for providing the support required to run the networks. Finally, suggestions made by three anonymous reviewers significantly improved this article.

## References

- Allen, R. M. (2007). The ElarmS earthquake early warning methodology and application across California, in *Earthquake Early Warning Systems*, P. Gasparini, G. Manfredi, and J. Zschau (Editors), Springer, Berlin, Heidelberg, 21–43.
- Allen, R. M., and H. Kanamori (2003). The potential for earthquake early warning in southern California, *Science* **300**, no. 5620, 786–789.
- Allen, R. M., P. Gasparini, O. Kamigaichi, and M. Bose (2009). The status of earthquake early warning around the world: An introductory overview, *Seismol. Res. Lett.* **80**, no. 5, 682–693.
- Anthony, R. E., A. T. Ringler, D. C. Wilson, and E. Wolin (2019). Do low-cost seismographs perform well enough for your network? An overview of laboratory tests and field observations of the OSOP Raspberry Shake 4D, *Seismol. Res. Lett.* **90**, no. 1, 219–228.
- Barrientos, S., and National Seismological Center (CSN) Team (2018). The seismic network of Chile, *Seismol. Res. Lett.* **89**, no. 2A, 467–474.
- Barrientos, S. E., S. Riquelme, and , and CSN Team (2021). Operational capabilities during crisis: The Chilean seismographic network, *Seismol. Res. Lett.* **92**, no. 1, 119–126.
- Béjar-Pizarro, M., A. Socquet, R. Armijo, D. Carrizo, J. Genrich, and M. Simons (2013). Andean structural control on interseismic coupling in the North Chile subduction zone, *Nature Geosci.* **6**, no. 6, 462–467.
- Böse, M., D. E. Smith, C. Felizardo, M. A. Meier, T. H. Heaton, and J. F. Clinton (2018). FinDer v. 2: Improved real-time ground-motion predictions for M2–M9 with seismic finite-source characterization, *Geophys. J. Int.* **212**, no. 1, 725–742.
- Brooks, B. A., M. Protti, T. Ericksen, J. Bunn, F. Vega, E. S. Cochran, C. Duncan, J. Avery, S. E. Minson, E. Chaves, *et al.* (2021). Robust earthquake early warning at a fraction of the cost: ASTUTI Costa Rica, *AGU Adv.* **2**, no. 3, e2021AV000407, doi: [10.1029/2021AV000407](https://doi.org/10.1029/2021AV000407).
- Chung, A. I., I. Henson, and R. M. Allen (2019). Optimizing earthquake early warning performance: ElarmS-3, *Seismol. Res. Lett.* **90**, no. 2A, 727–743.
- Comte, D., and M. Pardo (1991). Reappraisal of great historical earthquakes in the northern Chile and southern Peru seismic gaps, *Nat. Hazards* **4**, no. 1, 23–44.
- Cremen, G., and C. Galasso (2020). Earthquake early warning: Recent advances and perspectives, *Earth Sci. Rev.* **205**, 103184, doi: [10.1016/j.earscirev.2020.103184](https://doi.org/10.1016/j.earscirev.2020.103184).
- Crowell, B. W., D. A. Schmidt, P. Bodin, J. E. Vidale, B. Baker, S. Barrientos, and J. Geng (2018). G-FAST earthquake early warning potential for great earthquakes in Chile, *Seismol. Res. Lett.* **89**, no. 2A, 542–556.
- Derode, B., and J. Campos (2019). Energy budget of intermediate-depth earthquakes in northern Chile: Comparison with shallow earthquakes and implications of rupture velocity models used, *Geophys. Res. Lett.* **46**, no. 5, 2484–2493.
- Dziewonski, A. M., and D. L. Anderson (1981). Preliminary reference Earth model, *Phys. Earth Planet. Inter.* **25**, no. 4, 297–356.
- Finazzi, F., and A. Fasso (2017). A statistical approach to crowd-sourced smartphone-based earthquake early warning systems, *Stochastic Environ. Res. Risk Assess.* **31**, no. 7, 1649–1658.
- Hayes, G. P., M. W. Herman, W. D. Barnhart, K. P. Furlong, S. Riquelme, H. M. Benz, E. Bergman, S. Barrientos, P. Earle, and S. Samsonov (2014). Continuing megathrust earthquake potential in Chile after the 2014 Iquique earthquake, *Nature* **512**, no. 7514, 295–298.
- Hsiao, N. C., Y. M. Wu, T. C. Shin, L. Zhao, and T. L. Teng (2009). Development of earthquake early warning system in Taiwan, *Geophys. Res. Lett.* **36**, no. 5, doi: [10.1029/2008GL036596](https://doi.org/10.1029/2008GL036596).
- Husen, S., E. Kissling, E. Flueh, and G. Asch (1999). Accurate hypocentre determination in the seismogenic zone of the subducting Nazca Plate in northern Chile using a combined on-/offshore network, *Geophys. J. Int.* **138**, no. 3, 687–701.
- Kamigaichi, O., M. Saito, K. Doi, T. Matsumori, S. Y. Tsukada, K. Takeda, T. Shimoyama, K. Nakamura, M. Kiyomoto, and Y. Watanabe (2009). Earthquake early warning in Japan: Warning the general public and future prospects, *Seismol. Res. Lett.* **80**, no. 5, 717–726.
- Kausel, E., and J. Campos (1992). The Ms = 8 tensional earthquake of 9 December 1950 of northern Chile and its relation to the seismic potential of the region, *Phys. Earth Planet. In.* **72**, nos. 3/4, 220–235.
- Kurzon, I., R. N. Nof, M. Laporte, H. Lutzky, A. Polozov, D. Zakosky, H. Shulman, A. Goldenberg, B. Tatham, and Y. Hamiel (2020). The “TRUAA” seismic network: Upgrading the Israel seismic network—Toward national earthquake early warning system, *Seismol. Res. Lett.* **91**, no. 6, 3236–3255.
- Kuyuk, H. S., R. M. Allen, H. Brown, M. Hellweg, I. Henson, and D. Neuhauser (2014). Designing a network-based earthquake early warning algorithm for California: ElarmS-2, *Bull. Seismol. Soc. Am.* **104**, no. 1, 162–173.
- Lin, J. T., D. Melgar, A. M. Thomas, and J. Searcy (2021). Early warning for great earthquakes from characterization of crustal deformation patterns with deep learning, *J. Geophys. Res.* **126**, no. 10, e2021JB022703, doi: [10.1029/2021JB022703](https://doi.org/10.1029/2021JB022703).
- Lomnitz, C. (2004). Major earthquakes of Chile: A historical survey, 1535–1960, *Seismol. Res. Lett.* **75**, no. 3, 368–378.
- Massin, F., M. Böse, F. Suárez Bonilla, B. Burgoa Rosso, E. J. Chaves, J. Clinton, G. Marroquin, M. Protti, R. Racine, W. Strauch, *et al.* (2021). Towards earthquake early warning across Central America, *SSA 2021 Annual Meeting*, 1213–1479.
- Meier, M. A., Y. Kodera, M. Böse, A. Chung, M. Hoshiba, E. Cochran, S. Minson, E. Hauksson, and T. Heaton (2020). How often can earthquake early warning systems alert sites with high-intensity ground motion? *J. Geophys. Res.* **125**, no. 2, e2019JB017718, doi: [10.1029/2019JB017718](https://doi.org/10.1029/2019JB017718).
- Metois, M., C. Vigny, and A. Socquet (2016). Interseismic coupling, megathrust earthquakes and seismic swarms along the Chilean subduction zone (38–18 S), *Pure Appl. Geophys.* **173**, no. 5, 1431–1449.



- Peyrat, S., J. Campos, J. B. De Chabaliér, A. Pérez, S. Bonvalot, M. P. Bouin, D. Legrand, A. Necessian, O. Charade, G. Patau, *et al.* (2006). Tarapacá intermediate-depth earthquake (Mw 7.7, 2005, northern Chile): A slab-pull event with horizontal fault plane constrained from seismologic and geodetic observations, *Geophys. Res. Lett.* **33**, no. 22, doi: [10.1029/2006GL027710](https://doi.org/10.1029/2006GL027710).
- Riquelme, S., M. Medina, F. Bravo, S. Barrientos, J. Campos, and A. Cisternas (2018). W-phase real-time implementation and network expansion from 2012 to 2017: The experience in Chile, *Seismol. Res. Lett.* **89**, no. 6, 2237–2248.
- Ruiz, S., and R. Madariaga (2018). Historical and recent large megathrust earthquakes in Chile, *Tectonophysics* **733**, 37–56.
- Ruiz, S., M. Metois, A. Fuenzalida, J. Ruiz, F. Leyton, R. Grandin, C. Vigny, R. Madariaga, and J. Campos (2014). Intense foreshocks and a slow slip event preceded the 2014 Iquique Mw 8.1 earthquake, *Science* **345**, no. 6201, 1165–1169.
- Satriano, C., L. Elia, C. Martino, M. Lancieri, A. Zollo, and G. Iannaccone (2011). PRESTo, the earthquake early warning system for southern Italy: Concepts, capabilities and future perspectives, *Soil Dynam. Earthq. Eng.* **31**, no. 2, 137–153.

---

Manuscript received 17 November 2021

Published online 10 August 2022